

expected to influence the observed carrier densities (24). In going to the $m = 2$ structure, the layering of the perovskite structure results in the formation of terminal Sn-I interactions, which raise the Sn 5p antibonding (Sn-I) orbitals to higher energy, as well as reduce the band widths, resulting in a significant band gap (of order 0.5 eV). Increasing m leads to a progressive stabilization of the Sn 5p antibonding orbitals and a broadening of the Sn 5s and Sn 5p band widths, thereby effectively decreasing the band gap and leading to more metallic character. Notably, even for the metallic end-member of the series, $\text{CH}_3\text{NH}_3\text{SnI}_3$, the carrier density, measured by Hall effect (24), is only 2×10^{19} holes per cubic centimeter, which is two orders of magnitude smaller than in the superconducting bismuthate or cuprate perovskites. This, combined with the small effective mass ($m^* \approx 0.2$ for $\text{CH}_3\text{NH}_3\text{SnI}_3$), leads to a very small density of states at the Fermi energy, which (at least without doping) is not conducive to superconductivity.

Organic-inorganic multilayer materials, both self-assembling and artificially prepared, are particularly interesting because of the potential for tunability with respect to a given desired property. Artificially prepared organic-inorganic multilayers with interesting optoelectronic properties have, for example, been synthesized with the use of an ionized cluster beam apparatus with multiple ion sources (25). Self-assembling organic-inorganic perovskites offer the potential for tunability with, however, much simpler synthetic conditions than for the artificial structures.

Within the family of conducting tin iodide-based layered organic-inorganic perovskites, we have modified the orientation of the conducting perovskite layers through choice of organic cation. As with the {100} family of layered organic-inorganic perovskites, it is expected that the {110} structural family can accommodate a variety of different divalent metal halides, including the first-row transition-metal halides, and lead and cadmium halides, thereby providing additional interesting opportunities for the study of self-assembling multilayer quantum wells, two-dimensional magnetism, and optical, thermochromic, as well as transport properties. A preliminary demonstration of this is our recent synthesis, by the same technique described for the tin(II) compounds, of the lead(II) analog, which has monoclinic lattice parameters similar to those of the $m = 2$ tin compound but with a doubling of the basic unit cell along the b axis: $a = 6.315(3)$ Å, $b = 29.498(6)$ Å, $c = 8.713(1)$ Å, and $\beta = 90.96(3)^\circ$ (26).

REFERENCES AND NOTES

- G. V. Rubenacker, D. N. Haines, J. E. Drumheller, K. Emerson, *J. Magn. Magn. Mater.* **43**, 238 (1984).
- L. J. de Jongh and A. R. Miedema, *Adv. Phys.* **23**, 1 (1974).
- T. Ishihara, J. Takahashi, T. Goto, *Phys. Rev. B* **42**, 11099 (1990).
- J. Calabrese *et al.*, *J. Am. Chem. Soc.* **113**, 2328 (1991).
- M. F. Mostafa, M. M. Abdel-Kader, S. S. Arafat, E. M. Kandeel, *Phys. Scr.* **43**, 627 (1991).
- H. Arend, K. Tichy, K. Baberschke, F. Rys, *Solid State Commun.* **18**, 999 (1976).
- P. Day and R. D. Ledsham, *Mol. Cryst. Liq. Cryst.* **86**, 163 (1982).
- B. Tieke and G. Chapuis, *ibid.* **137**, 101 (1986).
- G. F. Needham, R. D. Willett, H. F. Franzen, *J. Phys. Chem.* **88**, 674 (1984).
- D. B. Mitzi, C. A. Feild, W. T. A. Harrison, A. M. Guloy, *Nature* **369**, 467 (1994).
- G. C. Papavassiliou, I. B. Koutselas, A. Terzis, M.-H. Whangbo, *Solid State Commun.* **91**, 695 (1994).
- R. A. Mohan Ram, P. Ganguly, C. N. R. Rao, *J. Solid State Chem.* **70**, 82 (1987).
- R. A. Mohan Ram, L. Ganapathi, P. Ganguly, C. N. R. Rao, *ibid.* **63**, 139 (1986).
- R. J. Cava *et al.*, *Phys. Rev. B* **46**, 14101 (1992).
- For $m = 2$, $\text{CH}_3\text{NH}_2\cdot\text{HI}$ (2.772 g, 17.44 mmol), NH_2CN (0.733 g, 17.44 mmol), and SnI_2 (6.495 g, 17.44 mmol) were dissolved in 70 ml of 57 weight % aqueous HI solution at 80°C. After soaking at 80°C for 12 hours, the solution was cooled to -10°C at 2°C/hour. The product was filtered under nitrogen, dried in flowing argon at 80°C for several hours, and then removed to an argon-filled dry box with oxygen and water levels maintained at <1 part per million. Powder x-ray diffraction indicated that the product was free of secondary phases such as

starting materials, $\text{CH}_3\text{NH}_3\text{SnI}_3$, and higher m members of the homologous series. Crystals of the $m = 3$ compound were grown with a similar technique but with a 2:5:5 molar ratio of NH_2CN , $\text{CH}_3\text{NH}_2\cdot\text{HI}$, and SnI_2 . The product contained a mixture of $m = 3$ and $\text{CH}_3\text{NH}_3\text{SnI}_3$. The sheet-like $m = 3$ crystals could be mechanically separated from the rod-like or rhombic dodecahedral cubic perovskite crystals because of the very different crystalline habit for these two materials. Isolated single crystals of $m = 4$ were similarly extracted from samples prepared in a solution containing a large excess of $\text{CH}_3\text{NH}_2\cdot\text{HI}$ and SnI_2 .

- E. N. Zil'berman, *Russ. Chem. Rev.* **31**, 615 (1962).
- M. L. Kilpatrick, *J. Am. Chem. Soc.* **69**, 40 (1947).
- D. Lin-Vien, N. B. Colthup, W. G. Fateley, J. G. Grasselli, Eds., *Handbook of Infrared and Raman Characteristic Frequencies of Organic Molecules* (Academic Press, New York, 1991).
- T. N. Sumarokova, R. A. Slavinskaya, I. G. Litvyak, Z. F. Orlova, *Russ. J. Inorg. Chem.* **13**, 561 (1968).
- L. J. Bellamy, *Infrared Spectra of Complex Molecules*, vol. 1 (Chapman and Hall, New York, 1986).
- M. Nanot, F. Queyroux, J.-C. Gilles, A. Carpy, J. Galy, *J. Solid State Chem.* **11**, 272 (1974).
- E. T. Keve, S. C. Abrahams, J. L. Bernstein, *J. Chem. Phys.* **53**, 3279 (1970).
- J. D. Donaldson and S. M. Grimes, *Rev. Silicon Germanium Tin Lead Compd.* **8**, 1 (1984).
- D. B. Mitzi, C. A. Feild, Z. Schlesinger, R. B. Laibowitz, *J. Solid State Chem.* **114**, 159 (1995).
- J. Takada, H. Awaji, M. Koshioka, A. Nakajima, W. A. Nevin, *Appl. Phys. Lett.* **61**, 2184 (1992).
- D. B. Mitzi, unpublished material.
- We thank T. Jackman, B. A. Scott, and A. Jacobson for stimulating discussions, and M. Ritter for use of a dispersive system for measuring the resistivity of these samples.

28 October 1994; accepted 9 January 1995

A "Double-Diamond Superlattice" Built Up of $\text{Cd}_{17}\text{S}_4(\text{SCH}_2\text{CH}_2\text{OH})_{26}$ Clusters

T. Vossmeier, G. Reck, L. Katsikas, E. T. K. Haupt, B. Schulz, H. Weller*

A simple preparation of $\text{Cd}_{17}\text{S}_4(\text{SCH}_2\text{CH}_2\text{OH})_{26}$ clusters in aqueous solution leads to the formation of colorless blocky crystals. X-ray structure determinations revealed a superlattice framework built up of covalently linked clusters. This superlattice is best described as two enlarged and interlaced diamond or zinc blende lattices. Because both the superlattice and the clusters display the same structural features, the crystal structure resembles the self-similarities known from fractal geometry. The optical spectrum of the cluster solution displays a sharp transition around 290 nanometers with a large absorption coefficient (~84,000 per molar per centimeter).

In the nanometer-size regime, the optical and transport properties of semiconductor clusters are controlled by the cluster size, whereas their chemical composition remains almost unchanged (1-6). For example, the optical properties of CdS nanoclusters change enormously with decreasing cluster size: The onset of absorption is shifted to higher energies, and the volume-normalized oscillator strength of the lowest electronic (excitonic) transition increases dramatically (7). These size effects result from the spatial confinement of the photo-generated charge carriers to the dimensions of the cluster, which can be represented by

the quantum mechanical model of a "particle in a box" (8). One of the most exciting questions is how solid-state properties develop when regular macroscopic structures are built up by the packing of clusters into a three-dimensional framework, as is fulfilled in crystallized cluster samples.

Because of cluster-cluster interactions, interesting collective phenomena are to be expected, and such well-structured systems should be useful for learning how quantum-size effects can be used for electronic devices. So far, only van der Waals or ionic crystals built up of CdS clusters, such as $\text{Cd}_{32}\text{S}_{14}(\text{SC}_6\text{H}_5)_{36} \cdot 4$ DMF (1)

(9) (DMF is *N,N*-dimethylformamide), $[\text{Cd}_{17}\text{S}_4(\text{SC}_6\text{H}_5)_{28}][\text{N}(\text{CH}_3)_4]_2$ (2) (10), and $[\text{Cd}_{10}(\text{SCH}_2\text{CH}_2\text{OH})_{16}][\text{SO}_4]_2 \cdot 4\text{H}_2\text{O}$ (3) (11), have been prepared. In this report, we present a single-crystal structure in which semiconductor clusters of CdS are linked covalently to build up a superlattice that is best described as consisting of two enlarged and interlaced diamond or zinc blende lattices. These lattices are identical and unlinked to each other. The same connective patterns are realized in both the macrostructure and the microstructure (superlattice and cluster, respectively), in a manner reminiscent of the self-similarities of fractal geometries. As we will show by ^{113}Cd nuclear magnetic resonance (NMR) and ultraviolet-visible (UVVIS) absorption measurements, the clusters remain intact after the crystals are dissolved in dimethyl sulfoxide (DMSO), DMF, or water.

The procedure of preparation has been described in principle (7). Briefly, cadmium perchlorate and 2-mercaptoethanol were dissolved in water, and H_2S was injected under vigorous stirring in alkaline solution (molar ratios of Cd:RS:S approximately 1.0:2.4:0.2) (*R* = alkyl). After it was stirred for several hours at room temperature, the solution was dialyzed exhaustively against water; then crystals began to grow in the dialysis tubes as small colorless needles while the solution reached a pH of 9. After dialysis, the crystals were stored in their mother liquor under reduced light because prolonged exposure to UV radiation leads to decomposition of the clusters. Upon standing for several weeks, blocky crystals grew on the bundles of needles, which themselves slowly decayed.

These crystals, which decompose above 160°C and are poorly soluble in water but readily soluble in DMF or DMSO, were used for x-ray structure analysis (12). Because the crystals cracked on drying, we found it necessary to carry out these measurements with a crystal enclosed in a thin glass tube containing a few microliters of mother liquor. The optical absorption properties (see below) of solutions of both crystal types (needles and blocks) were found to be the same, as were the solubilities. X-ray diffraction of

Fig. 1. The structures of the two $\text{Cd}_{17}\text{S}_4(\text{SCH}_2\text{CH}_2\text{OH})_{26}$ clusters that form the basic units of the superlattice. Both clusters 1 and 2 are chemically equivalent but crystallographically independent (see text). As can be seen, four capping thiolate ligands at the vertices of each cluster form a tetrahedron (edge lengths, 14.4 to 15.5 Å). These ligands act as intermolecular μ -SR

bridges and thus build up the superlattice framework. The Cd-(μ -SR) bonds have lengths between 2.48(1) and 2.60(1) Å (error in the last digit in parentheses). The intramolecular Cd-(μ -SR) bond lengths are similar and vary between 2.45(1) and 2.61(1) Å. The bond lengths between the central Cd atom and the four coordinating S atoms are also in the same range [2.48(1) to 2.53(1) Å].

the powdered needles revealed a strong amorphous background. Both crystal types are obviously built up of the same CdS clusters and differ from each other only in their crystal shape and in the degree of crystallinity. The total yield obtained (including both crystal types) was 31%, and the elemental analysis was in good agreement with the results of the structure analysis (13).

The basic unit that builds up the two interlaced superlattices is a cluster with the stoichiometry of $\text{Cd}_{17}\text{S}_4(\text{SCH}_2\text{CH}_2\text{OH})_{26}$ (4) (Fig. 1). This structure is similar to that of 2, which has been described by Dance and co-workers (10). If the cluster is considered as a part of the superlattice framework, it has the same approximate tetrahedral geometry (with exact D_2 symmetry) with open clefts running along each of the tetrahedral edges. These edges have a length between 14.4 and 15.5 Å. The CdS structure of the core is built up of four adamantanoid cages, sharing edges and one vertex, and may be regarded as a distorted fragment of the cubic CdS phase (zinc blende structure). However, the capping cages at each vertex are barrelanoid rather than adamantanoid and thus are more similar to the hexagonal (wurzite) phase than to the CdS (zinc blende) phase. The Cd-S bond lengths in the core are in the same range as for bulk CdS (2.519 Å) and vary between 2.45 and 2.61 Å.

Despite all of these similarities between 2 and 4, there is one decisive difference. Whereas 2 consists of negatively charged clusters with all vertices capped by terminating thiolate ligands to form an ionic cluster crystal, there are two ligands less in compound 4. Consequently, each cluster of the superlattice framework remains uncharged and is connected with four neighboring clusters by sharing each of its vertices. In other words, the four terminating thiolate ligands of 2 have been replaced in 4 by intermolecular μ -SR bridges between the clusters that

build up the superlattice framework.

The superlattice shown in Fig. 2 is best described chemically as two interlaced and enlarged diamond lattices. A more detailed description, however, shows that, within each diamond lattice, two chemically identical but crystallographically independent cluster species can be identified. Thus, the superlattice should be regarded crystallographically as two interlaced and enlarged zinc blende lattices. This feature is depicted in Fig. 3, which shows a comparison between a fraction of one of the interlacing superlattices (Fig. 3A) and an analogous portion of the zinc blende structure (Fig. 3B). The connectivity pattern is almost exactly the same for both structures. The angles differ only

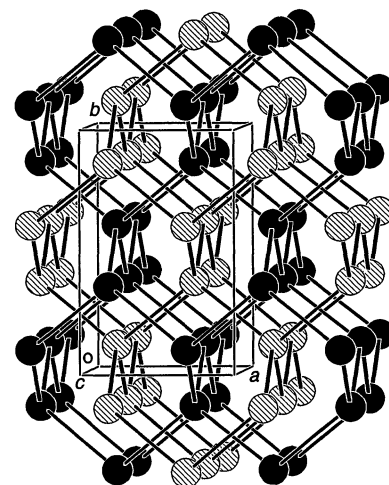
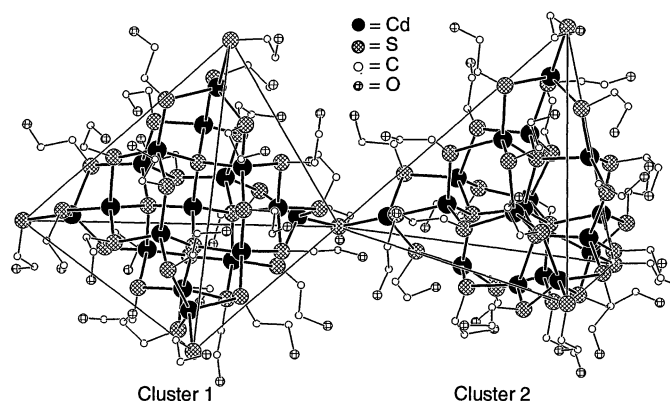


Fig. 2. The superlattice built up of the Cd_{17} clusters. This is best described as two enlarged and interlaced diamond (or zinc blende) lattices. Both lattices are identical and symmetry-related by the inversion center of the space group $I2/a$ with the fractional coordinates 0.25, 0.25, and 0.75. Only the central Cd atom of each cluster is depicted and connected with the other Cd atom. The monoclinic cell parameters are given in (12).

T. Vossmeier, Hahn-Meitner-Institut, Abteilung Kleinteilchenforschung, Glienicke Strasse 100, 14109 Berlin, Germany.

G. Reck and B. Schulz, Bundesanstalt für Materialforschung und -prüfung, Rudower Chaussee 5, 12489 Berlin, Germany.

L. Katsikas, University of Belgrade, Faculty of Technology and Metallurgy, Karnegijeva 4, 11000 Belgrade, Yugoslavia.

E. T. K. Haupt, Universität Hamburg, Institut für Anorganische und Angewandte Chemie, Martin-Luther-King-Platz 6, 20146 Hamburg, Germany.

H. Weller, Universität Hamburg, Institut für Physikalische Chemie, Bundesstrasse 45, 20146 Hamburg, Germany.

*To whom correspondence should be addressed.

slightly ($<8.6^\circ$), whereas the "bond lengths" differ by a factor of ~ 6.9 . Moreover, the structure of the cluster core (Fig. 3C) is similar to that of the superlattice framework, and it can be described as a fragment of the cubic CdS phase (zinc blende).

If the clusters remain intact upon dissolution (the prepared crystals dissolve poorly in water but readily in DMF or DMSO), only the intermolecular μ -SR bonds between the clusters are cleaved. This probably happens in such a manner that, on average, two vertices of each cluster are capped by a terminating thiolate ligand, whereas the other

two vertices remain uncapped. For NMR considerations the Cd atoms at the latter sites are expected to display a significant high field shift compared with the other Cd atoms, because they are coordinated by only three S atoms (14). Thus, the signal at 440 ppm, seen in the ^{113}Cd NMR spectrum of Fig. 4, is attributed to the two coordinatively unsaturated Cd atoms of these sites. At lower field, two other peaks are recognized: a strong signal at 630 ppm and a very weak one at 650 ppm. Because the chemical environment of the 12 Cd atoms at the cluster surfaces is similar to that of the two Cd atoms at the vertices, which are capped by a terminating thiolate ligand, the signals of these sites are probably superimposed around 630 ppm. The weak peak at 650 ppm is attributed to the central Cd, which is coordinated by the four inner S atoms.

Because of the relative abundance of surface Cd atoms and the low signal-to-noise ratio of the weak peaks, the relative intensities of the three signals are hard to compare. However, taking into account this limitation, the relative intensities given in Fig. 4 are in reasonable agreement with our interpretation. The Cd atoms that are coordinatively not saturated by S will be coordinated by solvent molecules (15) or in alkaline wa-

ter by OH^- ions. This explains the increasing solubility of **4** in water with increasing pH, as well as the reverse process of crystal formation in the dialysis tubings. As the pH value of an alkaline cluster solution decreases during dialysis, the thiolate S atoms of the two terminating ligands compete more successfully with OH^- ions for the two unsaturated coordination sites and finally form intermolecular μ -SR bridges between the clusters. This kind of polymerization leads to the crystal formation described above.

Because the thiolate ligand of **4** absorbs light only below 250 nm, the UVVIS spectrum of the cluster core could be investigated. Figure 5A shows spectra of solutions of the clusters in water, DMSO, and DMF. The well-pronounced absorption maximum around 290 nm is ascribed to the $1s1s$ excitonic transition. The molar absorption coefficient ($\epsilon_{290} \sim 84,000 \text{ M}^{-1} \text{ cm}^{-1}$), as well as the spectral position of the maximum, is almost independent of the solvent polarity. (B) Luminescence spectra of the crystalline solid (dotted line) and an aqueous solution (solid line) at 4 K. The excitation wavelength was 300 nm. The spectrum of the crystalline solid is slightly shifted to the red ($\sim 12 \text{ nm}$).

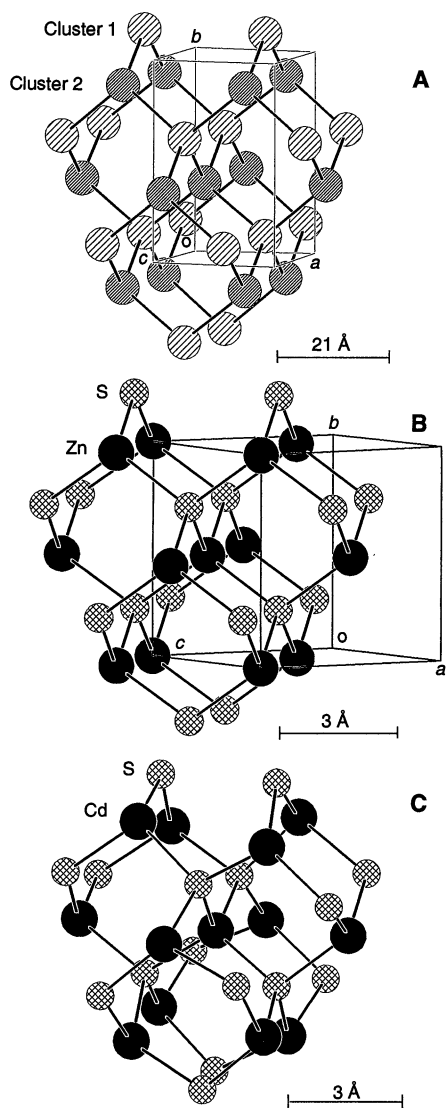


Fig. 3. Similarity between (A) the superlattice, (B) the zinc blende structure, and (C) the cluster core structure. In (A), the structure of one of the interlaced superlattices is depicted. In contrast to Fig. 2, in this figure the crystallographically different but chemically equal clusters are marked by different shadings (clusters 1 and 2). The unit cell refers to the whole structure and not only to the superlattice. Thus, the unit cells shown in (A) and (B) have different geometries. In (C), the capping vertices of the cluster are omitted. Note the scale bars of each part.

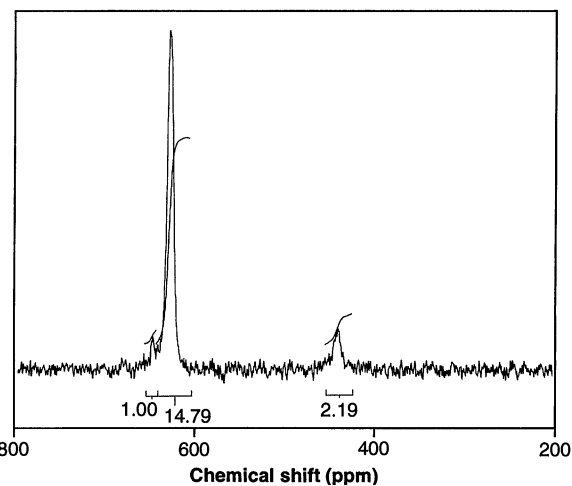


Fig. 4. A ^{113}Cd NMR spectrum recorded with a 0.06 M solution of **4** in $\text{DMSO-}d_6$. The relative intensities of the three signals at 650, 630, and 440 ppm are approximately 1:14.8:2.2. The spectrum was recorded with a Varian Gemini-200 BB-Spectrometer (4.7 T) at 44.4 MHz. We collected 53,200 pulses within 16 hours at room temperature (pulse width 45° , 1-s recycle delay). As a reference, $\delta_{\text{CdCl}_2} = 98 \text{ ppm}$ (1.0 M aqueous solution) was taken, which corresponds to $\delta_{\text{Cd-(ClO}_4)_2} = 0 \text{ ppm}$ (0.1 M aqueous solution) (16).

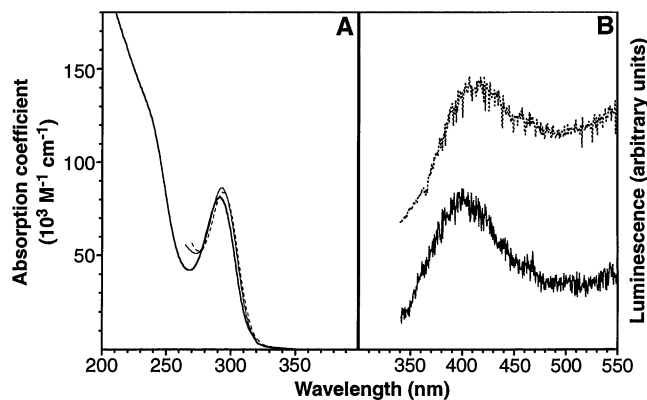


Fig. 5. (A) UVVIS spectra of **4** dissolved in different solvents (heavy line, water; light line, DMSO; dashed line, DMF). The transition near 290 nm has a large absorption coefficient ($\epsilon_{290} \sim 84,000 \text{ M}^{-1} \text{ cm}^{-1}$) and is almost independent of the solvent polarity. (B) Luminescence spectra of the crystalline solid (dotted line) and an aqueous solution (solid line) at 4 K. The excitation wavelength was 300 nm. The spectrum of the crystalline solid is slightly shifted to the red ($\sim 12 \text{ nm}$).

films, which were prepared on quartz plates by spin coating from concentrated cluster solutions, are similar to the spectrum of an aqueous solution. The position of the maximum is, however, shifted to the red by approximately 5 nm. The luminescence spectrum of the crystalline solid is also similar to the solution spectrum (Fig. 5B) and is also shifted slightly to the red (~12 nm). Thus, small optical changes that might reflect cluster-cluster interactions in the solid samples could be observed.

In (7) we described the synthesis and characterization of differently sized 1-thioglycerol-stabilized CdS clusters. One of the prepared species displayed exactly the same optical behavior as **4**. At that time, we speculated, on the basis of elemental analysis, small-angle x-ray scattering, and UV-VIS spectroscopy, that this sample might consist of Cd₁₇ clusters. However, attempts to crystallize this compound, which is readily water-soluble, have not been successful. Nevertheless, it should be possible to crystallize clusters of the type Cd₁₇S₄(RS)₂₆ with various thiolate ligands RS. This should lead to a set of different superlattices consisting of almost identical CdS cluster cores, which can be regarded as ideal systems for the study of collective phenomena based on cluster-cluster interactions.

REFERENCES AND NOTES

1. A. Henglein, *Top. Curr. Chem.* **143**, 113 (1988).
2. ———, *Chem. Rev.* **89**, 1861 (1989).
3. L. E. Brus, *Appl. Phys. A* **53**, 465 (1991).
4. Y. Wang and N. Herron, *J. Phys. Chem.* **95**, 525 (1991).
5. H. Weller, *Angew. Chem. Int. Ed. Engl.* **32**, 41 (1993).
6. ———, *Adv. Mater.* **5**, 88 (1993).
7. T. Vossmeier et al., *J. Phys. Chem.* **98**, 7665 (1994).
8. L. E. Brus, *ibid.* **80**, 4403 (1984).
9. N. Herron, J. C. Calabrese, W. E. Farneth, Y. Wang, *Science* **259**, 1426 (1993).
10. G. S. H. Lee et al., *J. Am. Chem. Soc.* **110**, 4863 (1988).
11. P. Strickler, *J. Chem. Soc. Chem. Commun.* **1969**, 655 (1969).
12. Diffraction data for the x-ray structure analysis were collected on an Enraf-Nonius (Delft, Netherlands) CAD4 diffractometer (graphite monochromatized MoK α radiation, wavelength of 0.7107 Å). The monoclinic cell parameters were determined from the Bragg angles of 25 computer-centered reflections as $a = 25.147(4)$ Å, $b = 40.096(5)$ Å, $c = 25.358(5)$ Å, and $\beta = 94.0(1)^\circ$ (error in the last digit in parentheses). The space group was assigned as $I2/a$ (no. 15), and the structure confirmed this assignment. The colorless, irregularly shaped crystals were very unstable, as indicated by the drastic loss in intensities during x-ray exposure. Therefore, three crystals (100 to 180 μm) sealed in capillaries were used for the data collection. Because of the instability and the weak diffraction power of the nonperfect crystals, only 5414 unique reflections with $I \geq 2\sigma(I)$ (where I is intensity) were measured in the range of $1.5^\circ \leq 2\theta \leq 38^\circ$ (θ is the dispersion angle). We solved the structure by direct methods and refined it by blocked full-matrix least squares techniques by using weighted restraints for the bond lengths and angles of the organic residues. Despite the poor quality of the available reflections, all C and O atoms could be located by difference Fourier synthesis. The final refinement of 587 parameters (data-to-parameter ratio = 9.2) in which only Cd was anisotropic converged at $R = 0.115$ (unit weights). This relatively high value may be attributable to the instability of the crystals, probably small structural changes during x-ray exposure, and rotational disorder of most of the organic residues indicated by the extreme high thermal parameters of some C and all O atoms. Additional data on this material can be ordered by referring to no. CSD-401359, names of the authors, and citation of the paper at the Fachinformationszentrum Karlsruhe, Gesellschaft für wissenschaftlich-technische Information mbH, D-76344 Eggenstein-Leopoldshafen, Germany.
13. Analysis calculated for C₅₂H₁₃₀O₂₆S₃₀Cd₁₇: C, 15.44%; H, 3.25%; O, 10.28%; S, 23.79%; and Cd, 47.24%. Found: C, 15.50%; H, 3.32%; O, 10.8%; S, 23.2%; and Cd, 46.5%.
14. R. A. Haberhorn et al., *Inorg. Chem.* **15**, 2408 (1976).
15. The observed signals of the ¹¹³Cd NMR spectrum, which are due to Cd atoms of the cluster surfaces and vertices (440 and 630 ppm) are most probably

broadened by exchange phenomena involving coordination by solvent molecules and OH groups of the organic residues. The involvement of OH groups is also indicated by ¹H NMR measurements; three temperature-dependent signals of hydroxyl protons were detected in DMF solution. The fact that the signal at 440 ppm could not be detected in DMF solution also indicates extensive exchange processes. However, because of the decreasing solubility of **4** in DMF with decreasing temperature, and decomposition at higher temperatures, no information could be obtained by temperature-dependent ¹¹³Cd NMR measurements.

16. A. D. Cardin, P. D. Ellis, J. D. Odom, J. W. Howard, *J. Am. Chem. Soc.* **97**, 1672 (1975).
17. We thank A. Mews for recording the luminescence spectra and A. Eychmüller for useful discussions.

30 August 1994; accepted 21 December 1994

Micrometer- and Nanometer-Sized Polymeric Light-Emitting Diodes

Magnus Granström,* Magnus Berggren, Olle Inganäs

A method for the fabrication of micrometer- and submicrometer-sized polymeric light-emitting diodes is presented. Such diodes have a variety of applications. Light sources of dimensions around 100 nanometers are required for subwavelength, near-field optical microscopy. Another possible application is patterning on the micrometer and nanometer scale. The diodes have been made in the form of a sandwich structure, with the conductive polymer poly(3,4-ethylene-dioxythiophene) polymerized in the pores of commercially available microfiltration membranes defining the hole-injecting contacts, poly[3-(4-octylphenyl)-2,2'-bithiophene] as the light-emitting layer, and a thin film of calcium-aluminum as the electron injector.

Since the first discoveries of electroluminescence in semiconducting conjugated polymers, interest has grown rapidly and many polymers have been used in light-emitting diodes (LEDs). The great interest is explained by the significant advantages that these systems have in processing, mechanical properties, and geometry possibilities as compared to conventional semiconductors (1–4). Another favorable aspect of the polymer LEDs is that today it is possible to cover the spectral range from blue to near-infrared, even within a single family of conductive polymers such as the polythiophenes (5). The recent demonstration of voltage-controlled electroluminescence colors from polymer blends in LEDs (5) as well as the possibility of obtaining polarized light from oriented polymers in LED devices (6) extend the possibilities of the polymer devices by comparison with inorganic devices. The mechanism for electroluminescence is also somewhat different from that found in conventional devices, because the emission takes place when charged po-

laron excitons recombine. When holes and electrons are injected into the polymer, they form positively and negatively charged polarons that can migrate under an applied field and radiatively recombine when they meet (7).

One of the advantages with polymer LEDs is the possibility to choose size and geometry freely. So far, this has mainly been exploited in making large (several square centimeters) LEDs. However, here we show that it is also possible to go in the other direction and make the light sources very small. Such LEDs could be used as light sources in scanning near-field optical microscopes (SNOMs), where the size of the emitting area is crucial (8, 9).

Two different conjugated polymers have been used in making these small LEDs. The first one, poly(3,4-ethylene-dioxythiophene) (10–13) (PEDOT) (1), was used as the hole-injecting contact; the other, poly[3-(4-octylphenyl)-2,2'-bithiophene] (14) (PTOPT) (2), was used as the electroluminescent layer (Fig. 1). To define the size of the light sources, we polymerized the doped and conducting polymer PEDOT electrochemically in the randomly distributed pores of commercially available microfiltration membranes (15, 16). The pore sizes in such mem-

Laboratory of Applied Physics, Department of Physics and Measurement Technology, Linköping University, S-581 83 Linköping, Sweden.

*To whom correspondence should be addressed.